

Article

Investigation of Catalytic Ozonation of Recalcitrant Organic Chemicals in Aqueous Solution over Various ZSM-5 Zeolites

Yandan Wang ^{1,†}, Wenfeng Ma ^{1,†}, Brandon A. Yoza ², Yingying Xu ¹, Qing X. Li ³,
Chunmao Chen ¹, Qinghong Wang ¹, Yu Gao ⁴, Shaohui Guo ¹ and Yali Zhan ^{1,*}

¹ State Key Laboratory of Petroleum Pollution Control, China University of Petroleum, Beijing 102249, China; donna.chan@163.com (Y.W.); mawenfeng234@163.com (W.M.); xuyingying1016@163.com (Y.X.); chunmaochan@163.com (C.C.); wangqhqh@163.com (Q.W.); cupgsh@163.com (S.G.)

² Hawaii Natural Energy Institute, University of Hawaii at Manoa, Honolulu, HI 96822, USA; byoza@hawaii.edu

³ Department of Molecular Biosciences and Bioengineering, University of Hawaii at Manoa, Honolulu, HI 96822, USA; qingli@hawaii.edu

⁴ College of Chemical and Environmental Engineering, Shandong University of Science and Technology, Qingdao 266590, China; daneycets@126.com

* Correspondence: wylzhan@cup.edu.cn; Tel.: +86-10-8973-3771

† These authors contributed equally to this work.

Received: 31 January 2018; Accepted: 20 March 2018; Published: 22 March 2018



Abstract: Catalytic ozonation processes (COPs) are an emerging technology for wastewater treatments. NaZSM-5 zeolites in three different SiO₂/Al₂O₃ ratios (31, 45, and 120) and their metallic oxides loaded samples were compared for COP of nitrobenzene solution. NaZSM-5(120) showed high total organic carbon (TOC) removals (70.2–74.0%) by adsorption relative to NaZSM-5(45) (0.4–0.6%) at various initial pH conditions. NaZSM-5(31) was obtained by NaOH treatment of NaZSM-5(45) and displayed 20.9–23.8% of TOC removals by adsorption. In COPs, the different ZSM-5 zeolites exhibited various TOC removals and different reaction pathways. COP-NaZSM-5(120) showed high TOC removals compared to COP-NaZSM-5(45) and COP-NaZSM-5(31). The repeated uses of zeolites in COPs were performed to understand the reaction pathways and contribution of adsorption versus ozonation (i.e., catalytic oxidation and/or direct ozonation). Both adsorption and direct ozonation in COP-NaZSM-5(120) contributed TOC removal for the first use, whereas direct ozonation and •OH mediated oxidation dominated the process for eight repeated uses. Direct ozonation and •OH-mediated oxidation controlled the COP-NaZSM-5(45) process for the first and eight repeated uses. Adsorption and direct ozonation governed the COP-NaZSM-5(31) process for the first use, whereas the direct ozonation dominated it for eight repeated uses. In COPs, NaZSM-5(120) and NaZSM-5(45) showed the catalytic activity, whereas NaZSM-5(31) displayed negligible catalytic activity. The high catalytic activity of NaZSM-5(120) may be due to more Si-O bonds on zeolite surfaces. The results revealed that loading of Mg oxide on ZSM-5 zeolites can increase catalytic activity in COPs. These results show the application potential of ZSM-5 zeolites in ozonation of recalcitrant chemical wastewaters.

Keywords: ozonation; ZSM-5 zeolites; SiO₂/Al₂O₃ ratios; nitrobenzene; adsorption

1. Introduction

The chemical industry produces large quantities of wastewater that contains various recalcitrant organic chemicals (ROCs). Catalytic ozonation processes (COPs) have been regarded as the most

promising and straightforward treatments due to its high efficiency [1–3]. A range of different catalysts are utilized for ROCs treatment in COPs including alumina [4], activated carbon [5], natural minerals [6,7], and metal oxides [8–10]. These catalysts can promote free radical (such as $\bullet\text{OH}$) formation from the decomposition of ozone, and further stimulate oxidation that increases the reaction rate [6,11,12]. Catalysts are also beneficial for the removal of other pollutants through adsorption [7]. For example, activated carbon can function as both an adsorbent and a catalyst for the treatment of benzenesulfonic acid and sulfanilic acid, through a complex mechanism that involves the direct ozonation, adsorption, and $\bullet\text{OH}$ oxidation that occurs at liquid and solid phase interfaces [5]. Pumice-loaded silicate can increase ozone mass transfer rates in aqueous solutions, and subsequently improved $\bullet\text{OH}$ generation, which resulted in increased mineralization of diclofenac [13].

Use of ZSM-5 zeolite as a catalyst for ozonation processes has attracted recent attention [11,14–16]. High-silica ZSM-5 has high adsorption capacities for ozone dissolved in water [15]. According to an investigation by Fujita et al., when high-silica ZSM-5 ($\text{SiO}_2/\text{Al}_2\text{O}_3 = 3000$) was used as a catalyst, it was effective at both concentrating ozone and other organic pollutants dissolved in water, resulting in significantly increased reaction rates [17,18]. Comparative studies using different ZSM-5 zeolites with various $\text{SiO}_2/\text{Al}_2\text{O}_3$ of 1000, 900, and 25 for the treatment of ROCs, exhibited enhanced ozonation activities [11,12,19,20]. High-silica ZSM-5 zeolites were found to be more efficient. The catalytic ozonation of organic pollutants on ZSM-5 zeolites results from the reaction of molecular ozone with pollutants adsorbed on the surface of zeolites [18]. The present investigation describes the importance of $\text{SiO}_2/\text{Al}_2\text{O}_3$ ratios of ZSM-5 zeolites when applied to COPs.

ZSM-5 zeolites had adjustable $\text{SiO}_2/\text{Al}_2\text{O}_3$ at about 10–3000, which impact their properties and applications [21,22]. Therefore, further investigation on ZSM-5 zeolite with more usual and available $\text{SiO}_2/\text{Al}_2\text{O}_3$ ranges is desirable and instructive in COP of ROCs. Our previous work found that the catalytic activity and reaction mechanism of activated carbon in the COP of refinery wastewater is masked due to the strong adsorption [23]. It is a question whether the natural function of ZSM-5 zeolites in COPs might also be due to adsorption. Additionally, carbon [24], Al_2O_3 [25], and MCM-41 [26] supporting metallic oxides have been used in COPs of ROCs. However, there were few reports on metallic oxides supported on ZSM-5 zeolites in COPs.

In this study, nitrobenzene is utilized as a model ROCs in this study. Three different $\text{SiO}_2/\text{Al}_2\text{O}_3$ ratios of NaZSM-5 zeolites (31, 45, and 120) and their metallic oxide-loaded samples were designed, characterized, and evaluated. The pathway for the removal of recalcitrant was simultaneously discussed. Additionally, the influence of the solution pH values on the efficiency of COPs of nitrobenzene in water was investigated with ZSM-5 zeolites. The surface active sites of ZSM-5 zeolites in COPs were firstly discussed.

2. Results and Discussion

2.1. Characteristics of Catalysts

Parent NaZSM-5 zeolites with the $\text{SiO}_2/\text{Al}_2\text{O}_3$ ratios at 120, 45 and 31 were abbreviated as pNaZSM-5(120), pNaZSM-5(45), and pNaZSM-5(31), respectively. The XRF (X-ray fluorospectrometer) results were used to confirm $\text{SiO}_2/\text{Al}_2\text{O}_3$ ratios of the pNaZSM-5(31), pNaZSM-5(45), and pNaZSM-5(120). The pNaZSM-5(31) had a low $\text{SiO}_2/\text{Al}_2\text{O}_3$ ratio relative to pNaZSM-5(45) due to desilication from the NaOH solution [27,28]. Similar surface morphologies and grain sizes were observed for pNaZSM-5(120), pNaZSM-5(45), and pNaZSM-5(31) (Figure 1). The pH_{pzc} values of pNaZSM-5(45), pNaZSM-5(120), and pNaZSM-5(31) were 9.7, 9.5, and 9.1, respectively. The loadings of Mg or Zn (0.87–0.93 wt%), as determined by XRF, agreed with the calculated values (0.9 wt%), demonstrating the efficiency of the incipient wetness impregnation methodology.

The pNaZSM-5(120), pNaZSM-5(45), and pNaZSM-5(31) had similar XRD patterns that were associated with the characteristic peaks of ZSM-5 zeolites [29]. Due to high dispersion and/or low concentrations, no obvious XRD diffraction peaks from the Mg or Zn oxides were observed (Figure 2a).

ZSM-5 zeolites exhibited typical FT-IR peaks of MFI structures at 1226 cm^{-1} , 1086 cm^{-1} , 796 cm^{-1} , 551 cm^{-1} , and 453 cm^{-1} (Figure 2b) [30]. The ZSM-5 zeolites were not significantly influenced by the loading of Mg or Zn oxides, accorded with the XRD results. The adsorption-desorption curves varied between the different ZSM5 zeolites (Figure 2c). According to IUPAC classification, the NaZSM-5(45) zeolites exhibited a typical micropore structure, while the NaZSM-5(120) and NaZSM-5(31) zeolites showed a mixed micropore-mesopore structure. The surface area and pore structure among the same series of ZSM-5 zeolites changed slightly (Table 1), probably due to the surface loading and/or better surface dispersion of metallic oxides [31]. NaZSM-5(120) and NaZSM-5(31) zeolites displayed high surface area and pore volume in comparison with NaZSM-5(45) zeolites (Table 1). The NaZSM-5(31) zeolites had an increased surface area and an unchanged micropore surface area compared to NaZSM-5(45) zeolites. These results are in accordance with a report by Ogura et al. [28].

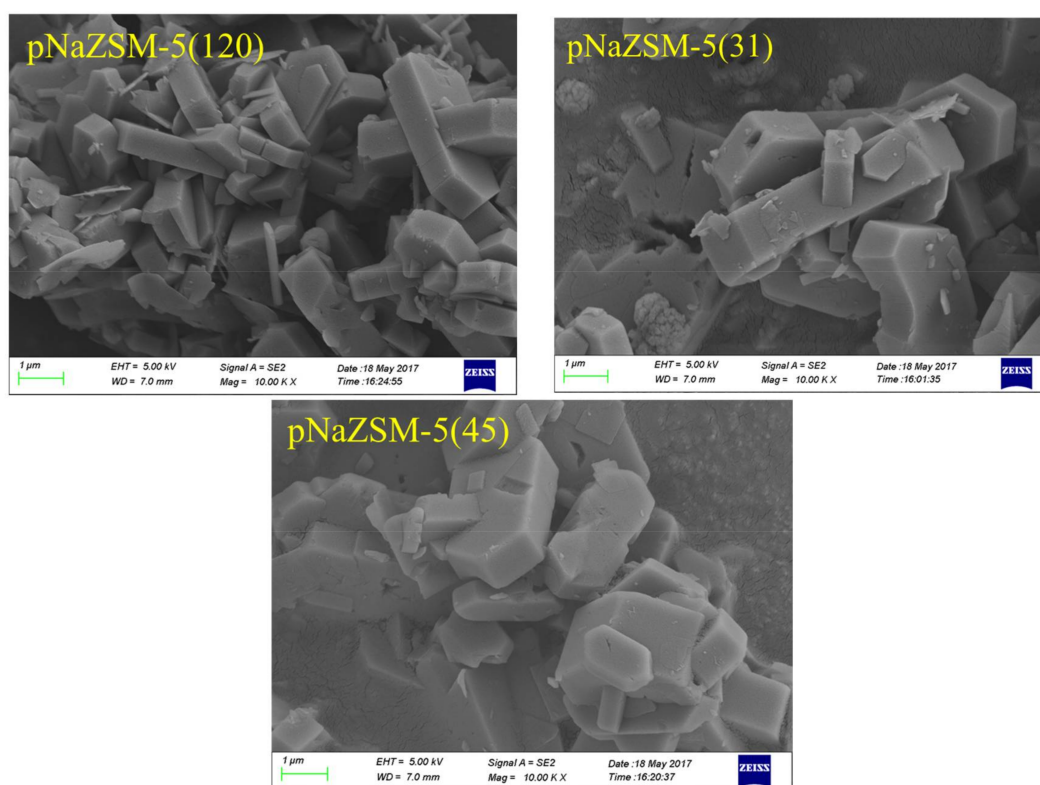


Figure 1. SEM images of pNaZSM-5(120), pNaZSM-5(45), and pNaZSM-5(31).

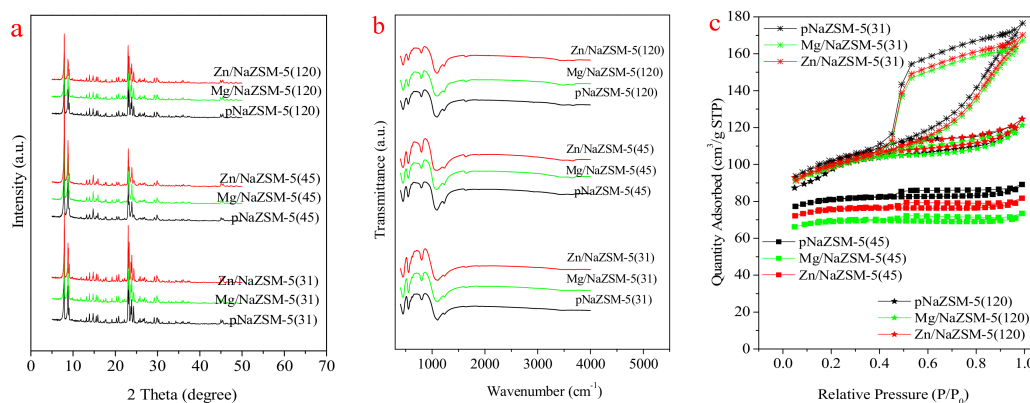
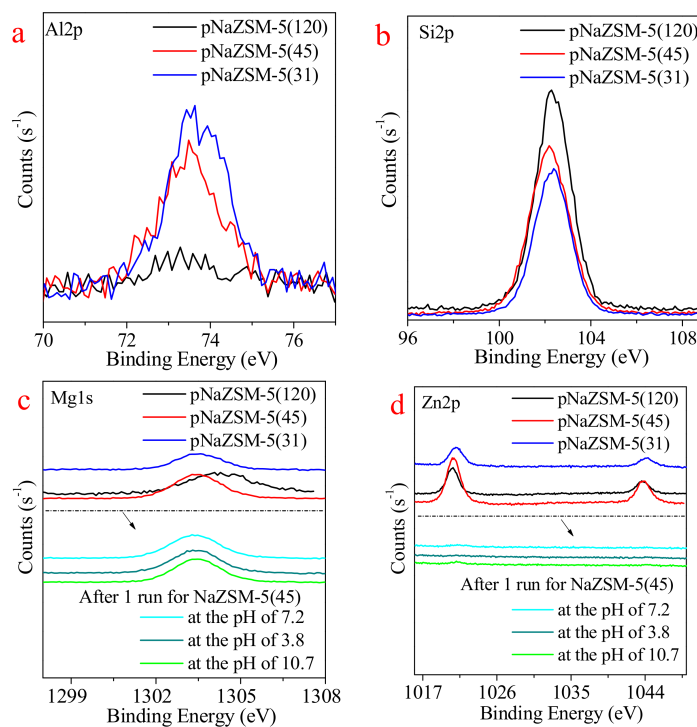


Figure 2. XRD patterns (a), FT-IR spectra (b), and adsorption-desorption isotherms (c) of ZSM-5 zeolites.

Table 1. Textural properties of NaZSM-5(120), NaZSM-5(45), and NaZSM-5(31) zeolites.

Zeolites	Surface Areas $\text{m}^2 \text{g}^{-1}$	Micropore Surface Areas $\text{m}^2 \text{g}^{-1}$	Total Pore Volumes $\text{cm}^3 \text{g}^{-1}$	Micropore Volumes $\text{cm}^3 \text{g}^{-1}$	Supported Metals Contents by XRF (wt%)
pNaZSM-5(120)	330	177	0.19	0.09	-
Mg/NaZSM-5(120)	324	223	0.19	0.11	0.94
Zn/NaZSM-5(120)	331	217	0.19	0.10	0.89
pNaZSM-5(45)	258	223	0.14	0.10	-
Mg/NaZSM-5(45)	223	200	0.11	0.10	0.90
Zn/NaZSM-5(45)	244	213	0.13	0.10	0.93
pNaZSM-5(31)	334	233	0.27	0.11	-
Mg/NaZSM-5(31)	326	237	0.27	0.11	0.87
Zn/NaZSM-5(31)	331	230	0.27	0.11	0.91

Figure 3a presented Al2p XPS spectra of pNaZSM-5(120), pNaZSM-5(45), and pNaZSM-5(31). The binding energy of Al2p from Al^{3+} oxides was concentrated at 74 eV [32]. Negligible Al2p XPS peak was observed for pNaZSM-5(120). The pNaZSM-5(31) showed a slightly high intensity of Al2p XPS peak relative to pNaZSM-5(45). Identical Si2p XPS peak was observed for pNaZSM-5(120), pNaZSM-5(45), and pNaZSM-5(31) at 102 eV (Figure 3b), mainly attributed to Si-O bonds in the framework of ZSM5 zeolites [33]. The intensity of Si2p XPS peak increases in an order of: pNaZSM-5(31) < pNaZSM-5(45) < pNaZSM-5(120). The NaOH modification promotes the surface Al content and slightly decreases the surface Si content of pNaZSM-5(45). The surface $\text{SiO}_2/\text{Al}_2\text{O}_3$ ratios of pNaZSM-5(120), pNaZSM-5(45), and pNaZSM-5(31) were almost infinite, 22.5 and 15.9, respectively, according to the XPS results. The changing trend of $\text{SiO}_2/\text{Al}_2\text{O}_3$ ratios of pNaZSM-5(120), pNaZSM-5(45), and pNaZSM-5(31) by XPS is supported by the XRF analysis. Figure 3c showed that Mg1s XPS peak from Mg^{2+} oxides at 1303–1305 eV for Mg loaded ZSM-5 zeolites [34]. The 2p XPS peak for Zn loaded ZSM-5 zeolites was located at 1021–1025 eV [35], associated to Zn^{2+} oxides (Figure 3d). The contents of Mg or Zn on NaZSM-5(120), NaZSM-5(45) and NaZSM-5(31) were 6.7 wt% or 5.9 wt%, 8.7 wt% or 9.5 wt%, and 5.6 wt% or 5.1 wt%, respectively, by XPS analysis. More surface metallic (Mg or Zn) oxides were dispersed on NaZSM-5(45) zeolites relative to NaZSM-5(31) and NaZSM-5(120) zeolites.

**Figure 3.** Al2p (a), Si2p (b), Mg1s (c), and Zn2p (d) XPS spectra of ZSM-5 zeolites.

2.2. TOC Removal of Nitrobenzene Solution in SAPs, SOP, and COPs

As determined by TOC analysis the removal of nitrobenzene using a single ozonation process (SOP) was lower when compared with the single adsorption process (SAP) and COP with NaZSM-5(120) zeolites (Figure 4). Adsorption for NaZSM-5(120) zeolites (SAP) reached saturation after 5 min, and had reduced TOC by 70.2–74.0% (Figure 4). The strong adsorption of nitrobenzene by NaZSM-5(120) zeolites is due to the high hydrophobicity of high-silica ZSM-5 zeolites [11,36]. The TOC removals (67.9–71.9%) were not time-dependent and were stable when used with COPs. NaZSM-5(120) zeolites-SAPs exhibited slightly higher TOC removals (about 2.0–4.3%) when compared with NaZSM-5(120) zeolite-COPs. These results suggest that TOC reduction is dependent only on the adsorptive capacity of NaZSM-5(120) zeolites instead of catalytic activity. There were only negligible differences of TOC removals from both SAPs and COPs with NaZSM-5(120) zeolites at different initial pH values. Mg- and Zn-loaded NaZSM-5(120) minimally impacted TOC removals in SAPs and COPs.

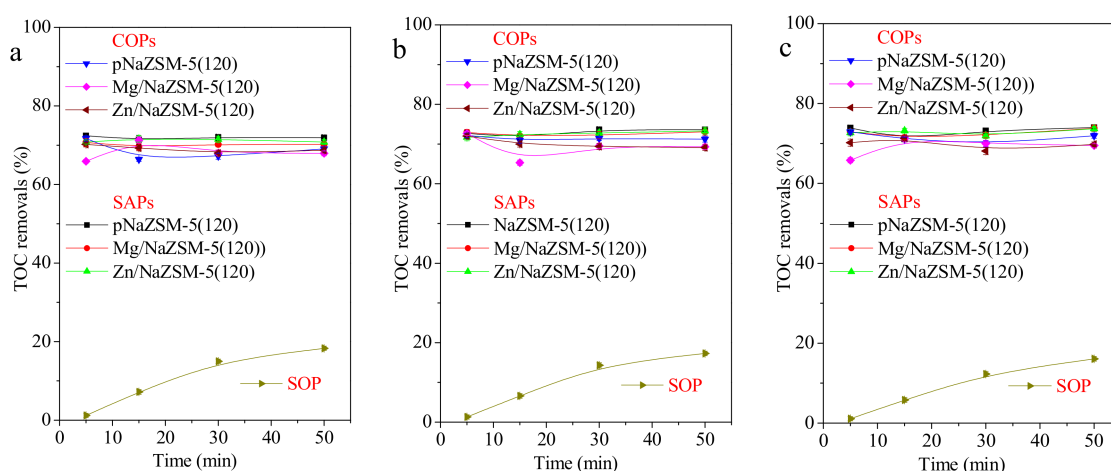


Figure 4. TOC removals during SOP, NaZSM-5(120) zeolites-SAPs and NaZSM-5(120) zeolite-COPs at different initial pH values of 3.8 (a), 7.2 (b), and 10.7 (c).

A small amount of TOC removals was achieved (0.4–0.6%) using NaZSM-5(45) zeolites-SAPs after 50 min treatment at different initial pH values (Figure 5). At the same initial pH, NaZSM-5(45) zeolite-COPs displayed higher TOC removals compared with SOP. NaZSM-5(45) zeolites had poor adsorption capability, and the catalytic activity of NaZSM-5(45) zeolites was responsible for the higher TOC removals. Mg/NaZSM-5(45)- and Zn/NaZSM-5(45) zeolite-COPs removed more TOC when compared with pNaZSM-5(45)-COP. Of the different NaZSM-5(45) zeolite-COPs, Mg/NaZSM-5(45)-COP was to most efficient at reducing TOC. This suggests that Mg oxide was the most effective active component examined. NaZSM-5(45) zeolite-COPs exhibited pH-dependency. NaZSM-5(45) zeolite-COPs were inhibited at higher initial pH (10.7) (Figure 5c). At the higher pH, the increased concentrations of hydroxide in aqueous suspension may decompose ozone [12,37]. Smaller differences for TOC removal occurred with initial pH values of 3.8 and 7.2 (Figure 5a,b).

Adsorption was saturated after 30 min using NaZSM-5(31) zeolites-SAPs and TOC removals (20.9–23.8%) were not influenced by pH (Figure 6). NaZSM-5(31) zeolites showed higher TOC removals when compared with NaZSM-5(45) zeolites in SAPs, due to high surface areas. At a pH of 3.8, the TOC removal was better for COP compared with SAP (Figure 6a). Adsorption and ozonation occurred during the catalytic ozonation treatments. However, the TOC removal in COP was less than the individual sums of SOP and SAP, due to competitive interactions between ozonation and adsorption. NaZSM-5(31) zeolite-COPs performed marginally better under acidic and neutral conditions relative to alkaline. Introduction of Mg or Zn oxides onto pNaZSM-5(31) improved TOC removals in COPs. Mg/NaZSM-5(31) exhibited slightly increased TOC removal when compared to Zn/NaZSM-5(31).

TOC removals using Mg/NaZSM-5(31)-COP was 30.9%, 33.4%, and 28.2% at initial pH values of 3.8, 7.2, and 10.7, respectively.

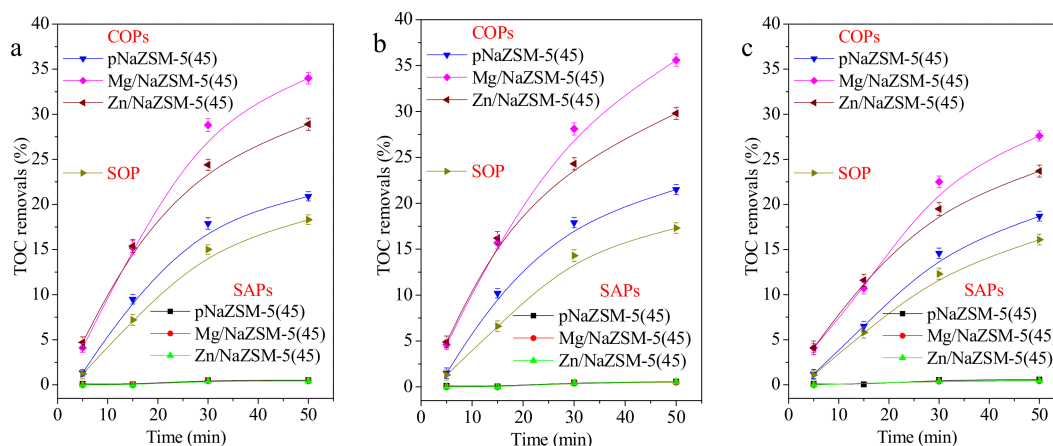


Figure 5. TOC removals during SOP, NaZSM-5(45) zeolites-SAPs and NaZSM-5(45) zeolite-COPs at initial pH values of 3.8 (a), 7.2 (b), and 10.7 (c).

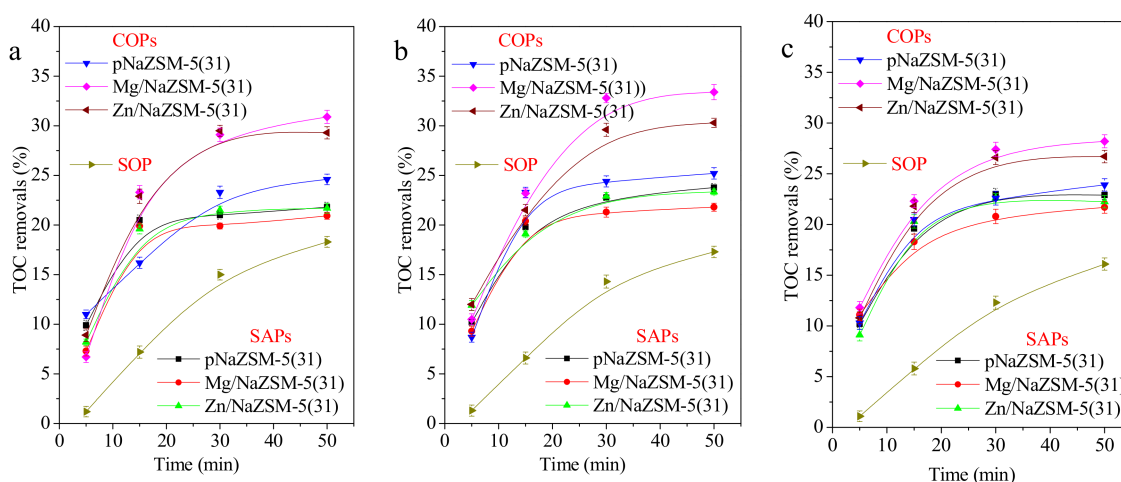


Figure 6. TOC removals during SOP, NaZSM-5(31) zeolites-SAPs and NaZSM-5(31) zeolite-COPs at initial pH values of 3.8 (a), 7.2 (b), and 10.7 (c).

TOC removals using ZSM-5s-COPs exhibited different mechanistic pathways; NaZSM-5(120) zeolite-COPs were dominated by adsorption, NaZSM-5(31) zeolite-COPs exhibited both ozonation and adsorption, and NaZSM-5(45) zeolite-COPs were controlled by ozonation. Adsorption with ZSM-5 impacts the effectiveness of catalytic ozonation for the removal of organic pollutants. Adsorption on the ZSM-5 assists in facilitating reactions with molecular ozone and pollutants on the surface of zeolites [11,15,16]. The adsorption capacity of NaZSM-5(120) zeolites and NaZSM-5(31) zeolite-COPs are well known. Among the examined ZSM-5s, only NaZSM-5(45) zeolites exhibited poor adsorption capacity. However, the introduction of Mg and Zn oxides on pNaZSM-5(45) further promoted its catalytic activity. This comparative study using NaZSM-5(120) zeolites, NaZSM-5(45) zeolites, and NaZSM-5(31) zeolite-COPs for nitrobenzene removal is useful for understanding the catalytic ozonation mechanisms using ZSM-5 zeolites.

2.3. Changes of Solution pH Values during SAP, SOP, and COP Treatments

Changes in the nitrobenzene solution pH values were used to determine the relationships between adsorption and ozonation. Changes in solution pH after a 50 min treatment during SOP, ZSM-5s-SAPs and ZSMs-COPs are shown in Figure 7. The SOP treatment resulted in a pH decrease from an initial 3.8 to 2.7. The ZSM-5s-SAPs treatment made the solution pH increasingly neutral (Figure 7a). The pH values after ZSM-5s-COPs treatment ranged between those values after SOP and ZSM-5s-SAPs (Figure 7a). At an initial pH of 7.2 and 10.7, similar trends were also observed (Figure 7b,c). These results suggest that both adsorption and ozonation contributed to TOC removal for ZSM-5s-COPs. These results also suggest that ozonation still occurs when using NaZSM-5(120) zeolite-COPs in spite of strong adsorption.

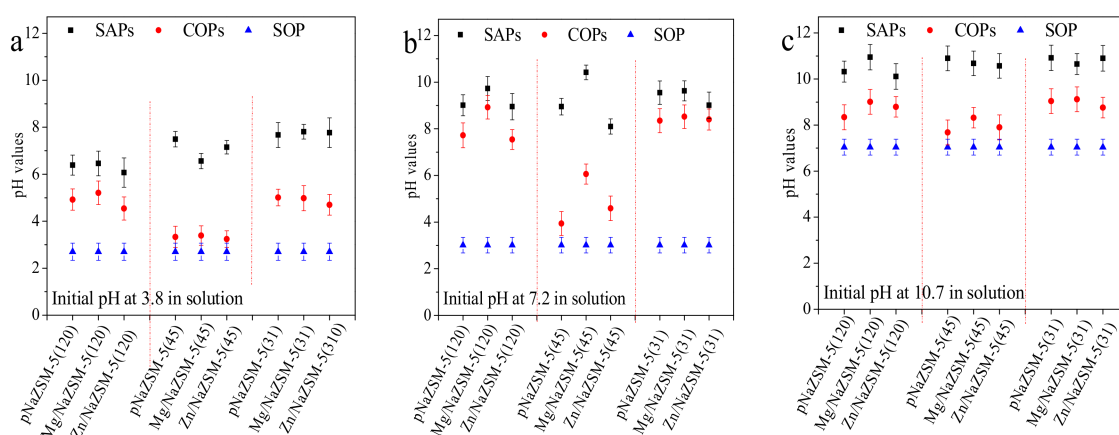


Figure 7. Changes of pH values of nitrobenzene solution after SOP, ZSM-5s-SAPs, and ZSM-5s-COPs treatments at initial pH values of 3.8 (a), 7.2 (b), and 10.7 (c).

2.4. Influences of Repeated Uses of Catalysts on COPs

The ZSM-5 zeolites were repeatedly used to determine its impact on adsorption [23]. The TOC removals by ZSMs-COPs at 50 min after each of the eight repeated uses are shown in Figure 8. The amount of TOC that was removed by NaZSM-5(120) zeolite-COPs gradually reduced (Figure 8a). The TOC removals by NaZSM-5(120) zeolite-COPs were 27.3–38.7% after the eighth use at an initial pH value of 3.8. However, the TOC removals were still higher when compared with SOP. The similar appearance happened in NaZSM-5(120) zeolite-COPs at the initial pH values of 7.2 and 10.7. This suggests the presence of catalytic activity for NaZSM-5(120) zeolites. The TOC removals by NaZSM-5(120) zeolite-COPs decreased after the 8th use; Mg/NaZSM-5(120) > Zn/NaZSM-5(120) \approx pNaZSM-5(120). The TOC removals by pNaZSM-5(45)-COP and Mg/NaZSM-5(45)-COP remained stable after repeated uses (Figure 8b) at the pHs. The TOC removals by Zn/NaZSM-5(45)-COP gradually decreased and was similar to those values obtained using pNaZSM-5(45)-COP. The TOC removed by NaZSM-5(31) zeolite-COPs gradually decreased with increased use (Figure 8c) at the pHs. After repeated use, the TOC removed by pNaZSM-5(31)-COP and Zn/NaZSM-5(31)-COP were only marginally better than SOP. The TOC removals of Mg/NaZSM-5(31)-COP increased by 6.2–9.6% compared to that of SOP.

It was found that after repeated uses, the catalytic activity of NaZSM-5(120) zeolites and Mg/NaZSM-5(31) is masked by adsorption until saturation. These results are in agreement with previous reports using activated carbon [23]. Among the ZSM-5s, pNaZSM-5(31) and Zn/NaZSM-5(31) displayed very weak catalytic ozonation activity. The Mg/NaZSM-5(120)-COP had the highest TOC removal capability (40.1%) at an initial pH value of 7.2 among ZSM-5s-COPs.

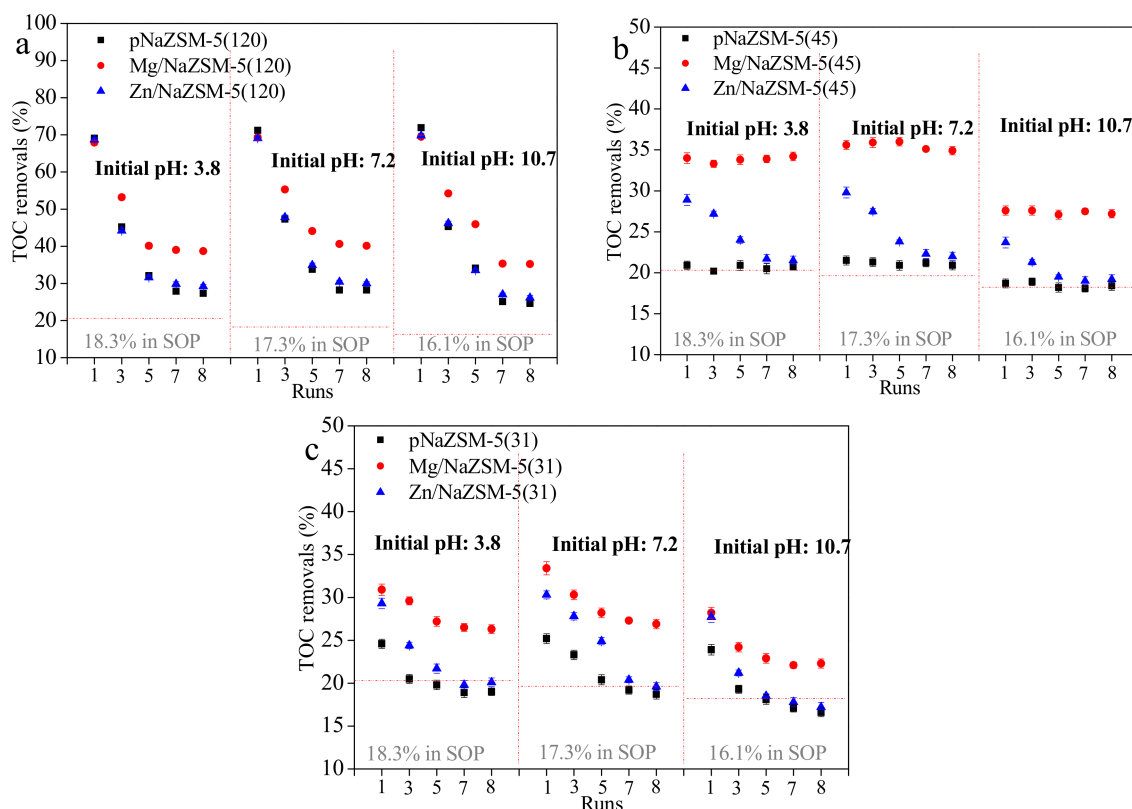


Figure 8. TOC removals after eight sequential uses in NaZSM-5(120) zeolite-COPs (a), NaZSM-5(45) zeolite-COPs (b), and NaZSM-5(31) zeolite-COPs (c) at various initial pH values.

A decrease in TOC removal efficiency was observed with catalytic ozonation using ZSM-5s supported by Zn oxide. Decreased efficiency was not observed with ZSM-5s supported by Mg oxide. The used and unused Mg/NaZSM-5(45) and Zn/NaZSM-5(45) zeolites were further analyzed by XPS (Figure 3c,d). After repeated use, Mg oxide remained and Zn oxide was nearly removed from the surface of NaZSM-5(45), as determined by XPS results. Similar results also occurred for Mg or Zn loaded NaZSM-5(120) and NaZSM-5(31). The decreased TOC removal with Zn loaded ZSM-5 zeolites potentially results from Zn oxide leaching from the surface of zeolites. The loading of Mg oxides on ZSM-5 zeolites effectively increases catalytic activity.

The catalytic activity of ZSM-5 zeolites is related to its surface properties. The surface atomic Si was dominant (31.6%) and no Al was detected for pNaZSM-5(120) (Figure 3b). The catalytic activity of pNaZSM-5(120) may originate from the surface Si-O bonds. The pNaZSM-5(45) showed a lower content of surface atomic Si (28.1%) relative to pNaZSM-5(120). The TOC removal of pNaZSM-5(45)-COP after repeated use was lower than those of pNaZSM-5(120)-COP. The TOC removal by pNaZSM-5(31)-COP was very low and close to that from SOP, suggesting weak catalytic activity for zeolite. The lowest surface atomic Si (27.2%) for pNaZSM-5(31) was observed relative to pNaZSM-5(45) and pNaZSM-5(120). Therefore, the surface Si-O bonds are original active sites of ZSM-5 zeolites. The loading of Mg or Zn oxides further increased active sites on the ZSM-5 zeolites.

2.5. Influences of NaHCO₃ on COPs

Sodium bicarbonate was used to determine the impact of $\bullet\text{OH}$ for the COP treatment of nitrobenzene in solution [38]. The TOC removals using NaZSM-5(120) zeolites- and NaZSM-5(31) zeolite-COPs during the first use remained unchanged after the addition of NaHCO₃ (Figure 9a). This suggests that direct ozonation and adsorption dominate these COPs. The TOC removal by NaZSM-5(45) zeolite-COPs was significantly decreased by the addition of NaHCO₃ (Figure 9a).

This suggests that under these conditions TOC is reduced by $\bullet\text{OH}$ mediated oxidation. However, TOC reductions still occurred in spite of NaHCO_3 introduction, which was a result of direct ozonation. These results suggest that direct ozonation and $\bullet\text{OH}$ mediated oxidation both occurred in NaZSM-5(45) zeolite-COPs.

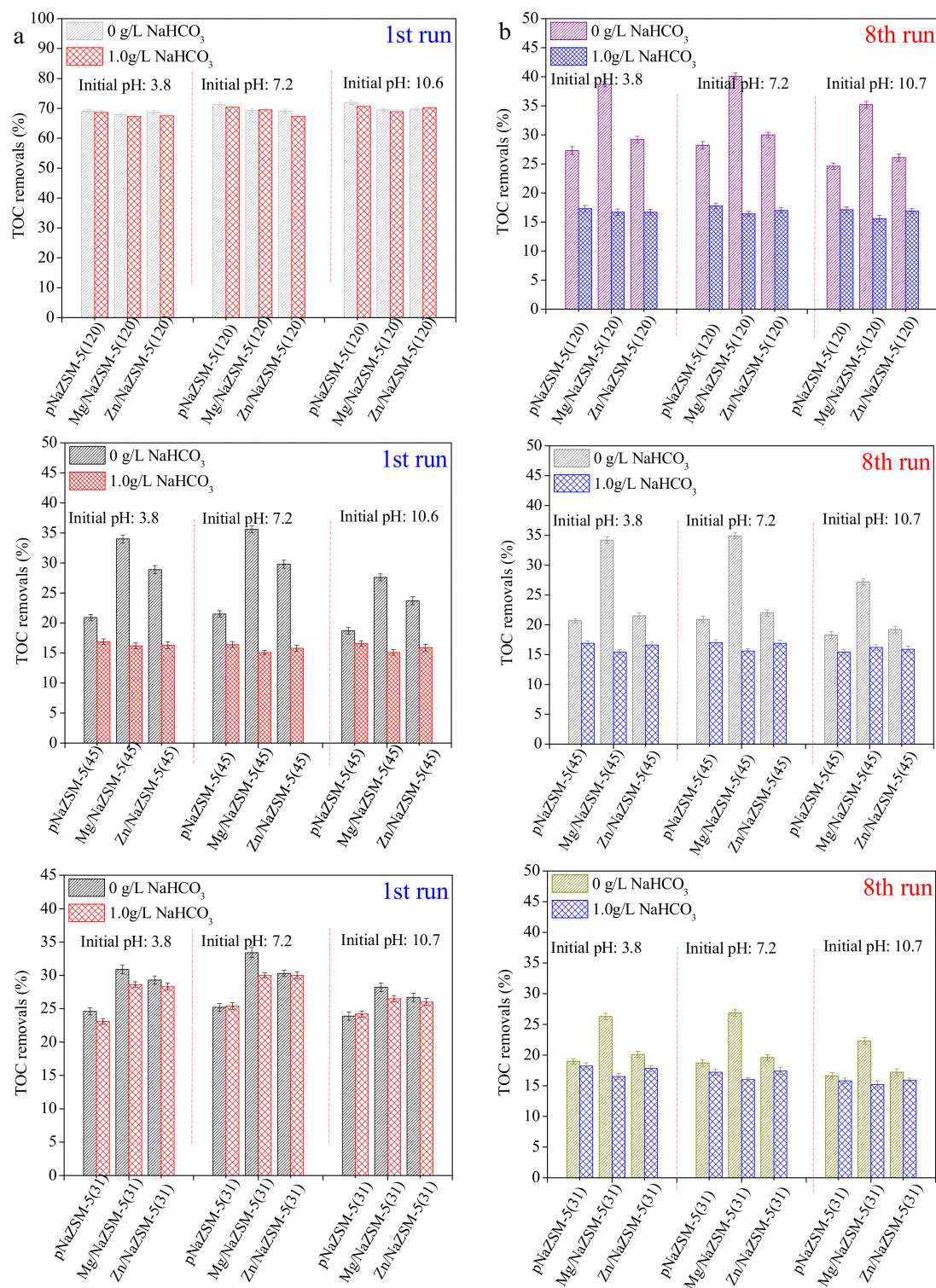


Figure 9. TOC removals of NaZSM-5(120) zeolites-, NaZSM-5(45) zeolites-, and NaZSM-5(31) zeolite-COPs in the first run (a) and eight run (b) at various initial pH values with or without NaHCO_3 addition.

The TOC removals of NaZSM-5(120) zeolite-COPs after eight uses significantly decreased by the addition of NaHCO_3 (Figure 9b), suggesting that $\bullet\text{OH}$ -mediated oxidation occurred. These results further expand the current mechanistic understanding for the use of high silica ZSM-5 during COP. These results show that there is a direct reaction of molecular ozone with the organic compounds that are adsorbed on the surface of zeolites. Similar reactions occur for the TOC removals by NaZSM-5(45) zeolite-COPs after the addition of NaHCO_3 (Figure 9b). For pNaZSM-5(31)-COP and Zn/NaZSM-5(31)-COP after the eight uses, a small decrease of TOC removal was observed after NaHCO_3 was introduced (Figure 9b). The results suggest the direct ozonation was the dominant process for pNaZSM-5(31)-COP and Zn/NaZSM-5(31)-COP. A reduction in the TOC removal by Mg/NaZSM-5(31)-COP after the eighth use was observed by NaHCO_3 introduction. This indicates that the $\bullet\text{OH}$ mediated oxidation and direct ozonation both regulated the COP.

The surface active sites of NaZSM-5(120) zeolites can produce active $\bullet\text{OH}$ s. The unstable $\bullet\text{OH}$ s need to rapidly react with nitrobenzene to avoid inactivation or reactions between themselves. The powerful adsorption of NaZSM-5(120) zeolites quickly decreases the nitrobenzene concentration in solution during its first use. Lower-concentrations of nitrobenzene decreases the probability of a reaction with $\bullet\text{OH}$ s. The catalytic activity of NaZSM-5(120) zeolites is masked under these conditions. Direct ozonation still occurs because the dissolved ozone in solution can react with the residual nitrobenzene. With increased use, the adsorption capacity of NaZSM-5(120) zeolites is gradually reduced by saturation. The adsorption function is reduced after repeated use and the nitrobenzene concentration in solution is high. The reactions between $\bullet\text{OH}$ s and nitrobenzene are enhanced after repeated use. The catalytic activity of NaZSM-5(120) zeolites in COPs appears, accordingly. For NaZSM-5(45) zeolite-COPs, the surface oxidation reactions are weak due to weak adsorption. The surface active sites of NaZSM-5(45) zeolites can decompose ozone to more active $\bullet\text{OH}$ s, which quickly react with nitrobenzene in solution, promoting TOC removal. Similar results were found in both the initial and after repeated use due to weak adsorption of NaZSM-5(45) zeolites. For pNaZSM-5(31)-COP, the adsorption is reduced after repeated use and weak catalytic capacity results in ineffective decomposition of ozone to $\bullet\text{OH}$ s. The pNaZSM-5(31)-COP was dominated by the direct ozonation after repeated use. Mg oxide on the surface of NaZSM-5(31) partially decomposes ozone to more active $\bullet\text{OH}$ s and promotes TOC removals during the COP.

3. Materials and Methods

3.1. Materials

The pNaZSM-5(120) and pNaZSM-5(45) were both purchased from Shanghai Sunny Molecular Sieve Plant, Shanghai, China. $\text{Mg}(\text{NO}_3)_2 \cdot 6\text{H}_2\text{O}$ (≥ 99.0 wt%), $\text{Zn}(\text{NO}_3)_2 \cdot 6\text{H}_2\text{O}$ (≥ 99.0 wt%), nitrobenzene (99.8 wt%), sodium bicarbonate (NaHCO_3), sodium hydroxide (NaOH) and hydrochloric acid (HCl) were all obtained from Beijing Chemical Reagents Co., Ltd., Beijing, China. Ultrapure water (18.2 m Ω /cm) was produced by a Direct-Pure UP ultrapure water system (Rephile Shanghai Bioscience Co., Ltd., Shanghai, China).

3.2. Preparation of Catalysts

A NaOH treatment for the ZSM-5 zeolites was used to decrease the $\text{SiO}_2/\text{Al}_2\text{O}_3$ ratios and increase functional surface areas [27,28]. The pNaZSM-5(31) was obtained by NaOH treated pNaZSM-5(45). It was prepared by adding 30 g of pNaZSM-5(45) into 600 g of NaOH solution (0.2 mol L^{-1}) at 363 K. This solution was stirred at 300 rpm for 4 h on a DF-101S magnetic stirrer (Gongyi Yuhua Instrument Co., Ltd., Gongyi, China). The suspension was then filtered using a FB-10T filter apparatus (Tianjin Automatic Science Co., Ltd., Tianjin, China) containing a 0.45 μm microfiltration membrane (Tianjin Jinteng Experimental Equipment Co., Ltd., Tianjin, China). The filtrate containing zeolites was washed using 1000 mL of ultrapure water and dried at 373 K for 12 h.

Metallic oxide loaded NaZSM-5 zeolites were prepared by an incipient wetness impregnation method. The 50 g of pNaZSM-5(120) was saturated with a solution containing 4.85 g $\text{Mg}(\text{NO}_3)_2 \cdot 6\text{H}_2\text{O}$ or 2.07 g $\text{Zn}(\text{NO}_3)_2 \cdot 6\text{H}_2\text{O}$. The impregnated sample was calcinated at 550 °C for 4 h in air after drying at 90 °C for 12 h to yield Mg/NaZSM-5(120) or Zn/NaZSM-5(120). The Mg/NaZSM-5(45), Zn/NaZSM-5(45), Mg/NaZSM-5(31), and Zn/NaZSM-5(31) were also prepared using this method.

3.3. Characterization of Catalysts

The crystals were observed by X-ray powder diffraction (XRD) with a XRD-6000 powder diffraction instrument (Shimadzu, Kyoto, Japan) with a 40.0 kV working voltage and 40.0-mA electric current. The surface area and pore volume were determined with an ASAP 2000 accelerated surface area and porosimetry system (Micromeritics, Norcross, GA, USA). The pH for point zero charge (pH_{pzc}) of the catalysts was determined according to the pH-drift procedure [39]. The composition was determined with a ZSX-100E X-ray fluorospectrometer (XRF) (Rigaku, Tokyo, Japan). The distribution of element deposition on the surface was recorded with a PHI Quantera SXM X-ray photoelectron spectrometer (XPS) (ULVAC-PHI, Chanhassen, MN, USA). The surface morphology was examined on a Quanta 200F scanning electron microscope (SEM). The functional groups on the surface were identified with a Magna-IR 560 ESP FT-IR spectrometer (Nicolet, Madison, WI, USA).

3.4. Ozonation of Nitrobenzene Solution

Nitrobenzene is one of the ubiquitous biological ROCs found in chemical wastewaters [40–43] and is, therefore, utilized as a model ROC in this study. The aqueous nitrobenzene solution was prepared at a concentration of 100 mg L^{-1} in ultrapure water. The initial TOC and pH values for 100 mg L^{-1} of nitrobenzene solution were 61.5 mg L^{-1} and 7.2, respectively.

The experimental system for the COP examination is illustrated in Figure 10. The system was constructed using: a 40 L of oxygen tank (Shandong Tianhai High Pressure Container, Co., Ltd., Linyi, China), a COM-AD-02 ozone generator (Anseros Advanced Oxidation Technologies Co., Ltd., Tübingen-Hirschau, Germany), two GM-6000-OEM ozone gas analyzers (Anseros Advanced Oxidation Technologies Co., Ltd., Tübingen-Hirschau, Germany), a D07-7 mass flow controller (Beijing Sevenstar Flow Co., Ltd., Beijing, China), a D08-1F flow readout box (Beijing Sevenstar Flow Co., Ltd., Beijing, China), a 1000 mL quartz column reactor and an exhaust gas collector. The reactor was placed on a ZNCL-BS intelligent magnetic stirrer (Shanghai Kankun Instrument Equipment Co., Ltd., Shanghai, China) at 800 rpm to ensure the efficient mass transfer of nitrobenzene, ozone, and catalyst.

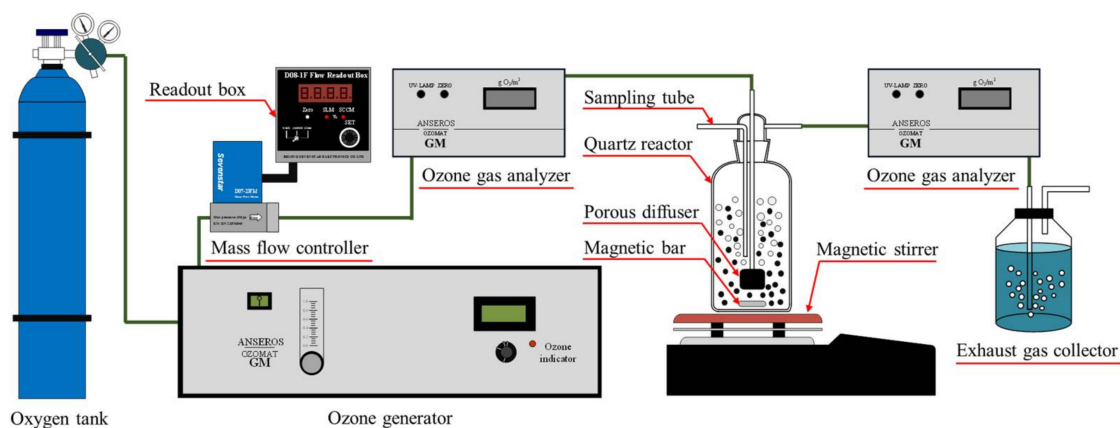


Figure 10. Flow diagram of COP experimental system.

During COP experimentation, an aliquot of 500 mL of nitrobenzene solution and 0.5 g of catalyst were added into the reactor at 30 °C. The gaseous ozone was then introduced through a porous diffuser

at the bottom of the reactor having a flow rate of 5 mg min^{-1} . A 10 mL aliquot of treated solution was then extracted using a 20 mL syringe. Catalyst particles were removed before further analysis by filtration using a $0.45 \text{ }\mu\text{m}$ syringe filter (Tianjin Jinteng Experimental Equipment Co., Ltd., Tianjin, China). The single adsorption process (SAP) was performed using the same experimental processes without ozone. The single ozonation process (SOP) was performed using the same experimental processes without ZSM-5 zeolites.

Oxidation mechanisms were determined through $\bullet\text{OH}$ quenching methods. NaHCO_3 was added into the nitrobenzene solution at a concentration of 1.0 g L^{-1} to scavenge free $\bullet\text{OH}$ prior to experimental use. Catalysis efficiencies were determined after the performance of eight replicates. After the first experimental run, the treated nitrobenzene solution containing catalyst was filtered through a FB-10T filter (Tianjin Automatic Science Instrument Co., Ltd., Tianjin, China) having a $0.45 \text{ }\mu\text{m}$ microfiltration membrane (Tianjin Jinteng Experimental Equipment Co., Ltd., Tianjin China). The catalyst containing filtrate was dried at $90 \text{ }^\circ\text{C}$ for 12 h, and the catalyst was reused. Between all subsequent experiments, 0.5 g catalyst was maintained by supplement of new catalyst before prior to use. All SAP, SOP, and COP experiments were performed in triplicate. The experiments were carried out using varying initial pH values (adjusted with 1 N NaOH or HCl). The pH and TOC values of the nitrobenzene solutions were measured with a MP 220 pH meter (Mettler Toledo, Greisensee, Switzerland) and a TOC-L CPH CN 200 TOC analyzer (Shimadzu, Kyoto, Japan).

4. Conclusions

Three different $\text{SiO}_2/\text{Al}_2\text{O}_3$ ratios of NaZSM-5 zeolites (31, 45, and 120) and their metallic oxide were investigated using COP for the treatment of nitrobenzene in solution. NaZSM-5(120) exhibited high TOC removal capabilities (70.2–74.0%) by adsorption, relative to NaZSM-5(45) (0.4–0.6%) at different initial pH values. NaZSM-5(31) was produced by treating NaZSM-5(45) with NaOH and was able to remove 20.9–23.8% of TOC by adsorption. The comparative study using NaZSM-5(120), NaZSM-5(45), and NaZSM-5(31) in COPs for the removal of nitrobenzene from solution expands the current understanding of mechanisms that occur during COPs with ZSM-5 zeolites. High TOC removals were obtained in ZSM-5-aided COPs under acidic and neutral conditions compared with alkaline. The compared ZSM-5 zeolites had different TOC removal capabilities and also different reactions COP treatment. NaZSM-5(120) was more efficient at removing TOC when compared with NaZSM-5(45) and NaZSM-5(31). For NaZSM-5(120), the adsorption and direct ozonation jointly contributed toward the reduction of TOC during its first use. Subsequent use proceeded to remove TOC by direct ozonation and $\bullet\text{OH}$ mediated oxidation. For NaZSM-5(45), direct ozonation and $\bullet\text{OH}$ mediated oxidation controlled the process for the first and subsequent uses. For NaZSM-5(31), adsorption and direct ozonation occurred during its initial application and subsequent application by direct ozonation. NaZSM-5(120) and NaZSM-5(45) exhibited catalytic activity, while NaZSM-5(31) did not. The high catalytic activity of NaZSM-5(120) may be due to more surface Si-O bonds for zeolite. The loading of Mg oxide on ZSM-5 zeolites can increase catalytic ozonation activity. These results show the potential of ZSM-5 zeolites and describe the reaction mechanisms for ozonation of recalcitrant chemical wastewaters.

Acknowledgments: This project was supported in part by the National Science and Technology Major Project of China (no. 2016ZX05040-003), the National Natural Science Foundation of China (no. 21776307), and the US Office of Naval Research (grants N00014-09-1-0709 and N00014-12-1-0496 284).

Author Contributions: Y.Z. and Y.W. conceived and designed the experiments; W.M. and Y.X. performed the experiments; B.A.Y., C.C., and Q.X.L. interpreted and analyzed the data; Y.G. and Q.W. contributed reagents/materials/analysis tools; and Y.W., B.A.Y., Q.X.L. and S.G. wrote the manuscript.

Conflicts of Interest: The authors declare no conflict of interest.

References

1. Lin, Y.; Han, X.; Lu, H.; Zhou, J. Study of archaea community structure during the biodegradation process of nitrobenzene wastewater in an anaerobic baffled reactor. *Int. Biodeter. Biodegr.* **2013**, *85*, 499–505. [[CrossRef](#)]
2. Qi, F.; Xu, B.; Chen, Z.; Feng, L.; Zhang, L.; Sun, D. Catalytic ozonation of 2-isopropyl-3-methoxypyrazine in water by γ -AlOOH and γ -Al₂O₃: Comparison of removal efficiency and mechanism. *Chem. Eng. J.* **2013**, *219*, 527–536. [[CrossRef](#)]
3. Dai, Q.; Wang, J.; Chen, J.; Chen, J. Ozonation catalyzed by cerium supported on activated carbon for the degradation of typical pharmaceutical wastewater. *Sep. Purif. Technol.* **2014**, *127*, 112–120. [[CrossRef](#)]
4. He, Z.; Zhang, A.; Song, S.; Liu, Z.; Chen, J.; Xu, X.; Liu, W. γ -Al₂O₃ modified with praseodymium: an application in the heterogeneous catalytic ozonation of succinic acid in aqueous solution. *Ind. Eng. Chem. Res.* **2010**, *49*, 12345–12351. [[CrossRef](#)]
5. Faria, P.; Órfão, J.; Pereira, M. Catalytic ozonation of sulfonated aromatic compounds in the presence of activated carbon. *Appl. Catal. B Environ.* **2008**, *83*, 150–159. [[CrossRef](#)]
6. Wu, J.; Ma, L.; Chen, Y.; Cheng, Y.; Liu, Y.; Zha, X. Catalytic ozonation of organic pollutants from bio-treated dyeing and finishing wastewater using recycled waste iron shavings as a catalyst: Removal and pathways. *Water Res.* **2016**, *92*, 140–148. [[CrossRef](#)] [[PubMed](#)]
7. Zhang, T.; Ma, J. Catalytic ozonation of trace nitrobenzene in water with synthetic goethite. *J. Mol. Catal. A Chem.* **2008**, *279*, 82–89. [[CrossRef](#)]
8. Wang, J.; Bai, Z. Fe-based catalysts for heterogeneous catalytic ozonation of emerging contaminants in water and wastewater. *Chem. Eng. J.* **2017**, *312*, 79–98. [[CrossRef](#)]
9. Radhakrishnan, R.; Oyama, S.T. Ozone decomposition over manganese oxide supported on ZrO₂ and TiO₂: A kinetic study using in situ laser Raman spectroscopy. *J. Catal.* **2001**, *199*, 282–290. [[CrossRef](#)]
10. Hu, C.; Xing, S.; Qu, J.; He, H. Catalytic ozonation of herbicide 2, 4-D over cobalt oxide supported on mesoporous zirconia. *J. Phys. Chem. C* **2008**, *112*, 5978–5983. [[CrossRef](#)]
11. Ikhlaga, A.; Brown, D.R.; Kasprzyk-Hordern, B. Catalytic ozonation of chlorinated VOCs on ZSM-5 zeolites and alumina: Formation of chlorides. *Appl. Catal. B Environ.* **2017**, *200*, 274–282. [[CrossRef](#)]
12. Ikhlaga, A.; Brown, D.R.; Kasprzyk-Hordern, B. Mechanisms of catalytic ozonation on alumina and zeolites in water: Formation of hydroxyl radicals. *Appl. Catal. B Environ.* **2012**, *123–124*, 94–106. [[CrossRef](#)]
13. Gao, G.; Shen, J.; Chu, W.; Chen, Z.; Yuan, L. Mechanism of enhanced diclofenac mineralization by catalytic ozonation over iron silicate-loaded pumice. *Sep. Purif. Technol.* **2017**, *173*, 55–62. [[CrossRef](#)]
14. Amin, N.A.S.; Akhtar, J.; Rai, H.K. Screening of combined zeolite-ozone system for phenol and COD removal. *Chem. Eng. J.* **2010**, *158*, 520–527. [[CrossRef](#)]
15. Fujita, H.; Izumi, J.; Sagehashi, M.; Fujii, T.; Sakoda, A. Adsorption and decomposition of water-dissolved ozone on high silica zeolites. *Water Res.* **2004**, *38*, 159–165. [[CrossRef](#)]
16. Rajasekhar Pullabhotla, V.S.R.; Jonnalagadda, S.B. Scope of metal loaded microporous ZSM-5 zeolites in the “catazone” process of n-hexadecane at moderate conditions. *Ind. Eng. Chem. Res.* **2009**, *48*, 9097–9105. [[CrossRef](#)]
17. Fujita, H.; Izumi, J.; Sagehashi, M.; Fujii, T.; Sakoda, A. Decomposition of trichloroethene on ozone-adsorbed high silica zeolites. *Water Res.* **2004**, *38*, 166–172. [[CrossRef](#)]
18. Fujita, H.; Shiraiishi, K.; Fujii, T.; Sakoda, A.; Izumi, J. Adsorbed phase ozonation of water-dissolved organic pollutants using high-silica zeolites. *Adsorption* **2005**, *11*, 835–839. [[CrossRef](#)]
19. Ikhlaga, A.; Brown, D.R.; Kasprzyk-Hordern, B. Catalytic ozonation for the removal of organic contaminants in water on ZSM-5 zeolites. *Appl. Catal. B Environ.* **2014**, *154–155*, 110–122. [[CrossRef](#)]
20. Ikhlaga, A.; Brown, D.R.; Kasprzyk-Hordern, B. Mechanisms of catalytic ozonation: An investigation into superoxide ion radical and hydrogen peroxide formation during catalytic ozonation on alumina and zeolites in water. *Appl. Catal. B Environ.* **2013**, *129*, 437–449. [[CrossRef](#)]
21. Xu, R.; Pang, W. *Chemistry-Zeolites and Porous Materials*, 2nd ed.; Science Press: Beijing, China, 2004; pp. 5–15.

22. Armaroli, T.; Simon, L.J.; Digne, M.; Montanari, T.; Bevilacqua, M.; Valtchev, V.; Patarin, J.; Busca, G. Effects of crystal size and Si/Al ratio on the surface properties of H-ZSM-5 zeolites. *Appl. Catal. A Gen.* **2006**, *36*, 78–84. [[CrossRef](#)]
23. Chen, C.; Wei, L.; Guo, X.; Guo, S.; Yan, G. Investigation of heavy oil refinery wastewater treatment by integrated ozone and activated carbon-supported manganese oxides. *Fuel Process. Technol.* **2014**, *124*, 165–173. [[CrossRef](#)]
24. Faria, P.C.C.; Órfão, J.J.M.; Pereir, M.F.R. A novel ceria-activated carbon composite for the catalytic ozonation of carboxylic acids. *Catal. Commun.* **2008**, *9*, 2121–2126. [[CrossRef](#)]
25. Chen, C.; Chen, Y.; Yoza, B.A.; Du, Y.; Wang, Y.; Li, Q.X.; Yi, L.; Guo, S.; Wang, Q. Comparison of Efficiencies and Mechanisms of Catalytic Ozonation of Recalcitrant Petroleum Refinery Wastewater by Ce, Mg, and Ce-Mg Oxides Loaded Al₂O₃. *Catalysts* **2017**, *7*, 72. [[CrossRef](#)]
26. Huang, R.; Lan, B.; Chen, Z.; Yan, H.; Zhang, Q.; Li, L. Catalytic ozonation of p-chlorobenzoic acid over MCM-41 and Fe loaded MCM-41. *Chem. Eng. J.* **2012**, *180*, 19–24. [[CrossRef](#)]
27. Groen, J.C.; Peffer, L.A.A.; Moulijin, J.A.; Pérez-Ramírez, J. Mesoporosity development in ZSM-5 zeolite upon optimized desilication conditions in alkaline medium. *Colloids Surf. A* **2004**, *241*, 53–58. [[CrossRef](#)]
28. Ogura, M.; Shinomiya, S.; Tateno, J.; Nara, Y. Alkali-treatment technique-new method for modification of structural and acid-catalytic properties of ZSM-5 zeolites. *Appl. Catal. A Gen.* **2001**, *219*, 33–43. [[CrossRef](#)]
29. Huang, X.; Yuan, J.; Shi, J.; Shangguan, W. Ozone-assisted photocatalytic oxidation of gaseous acetaldehyde on TiO₂/H-ZSM-5 catalysts. *J. Hazard. Mater.* **2009**, *171*, 827–832. [[CrossRef](#)] [[PubMed](#)]
30. Zhao, X.; Wei, L.; Cheng, S.; Cao, Y.; Julson, J.; Gu, Z. Catalytic cracking of carinata oil for hydrocarbon biofuel over fresh and regenerated Zn/Na-ZSM-5. *Appl. Catal. A Gen.* **2015**, *507*, 44–55. [[CrossRef](#)]
31. Huang, H.B.; Huang, W.; Xu, Y.; Ye, X.; Wu, M.; Shao, Q.; Ou, G.; Peng, Z.; Shi, J.; Chen, J.; et al. Catalytic oxidation of gaseous benzene with ozone overzeolite-supported metal oxide nanoparticles at room temperature. *Catal. Today* **2015**, *258*, 627–633. [[CrossRef](#)]
32. Suib, S.L.; Winiecki, A.M.; Kostapapas, A. Surface states of aluminophosphate and zeolite molecular sieves. *Stud. Surf. Sci. Catal.* **1986**, *28*, 409–414.
33. Ismail, M.N.; Goodrich, T.L.; Ji, Z.; Ziemer, K.S.; Warzywoda, J.; Sacco, A., Jr. Assembly of titanosilicate ETS-10 crystals on organosilane-functionalized gallium nitride surfaces. *Micropore Mesopor. Mater.* **2009**, *118*, 245–250. [[CrossRef](#)]
34. Moussavi, G.; Aghapour, A.A.; Yaghmaeian, K. The degradation and mineralization of catechol using ozonation catalyzed with MgO/GAC composite in a fluidized bed reactor. *Chem. Eng. J.* **2014**, *249*, 302–310. [[CrossRef](#)]
35. Gallegos, M.V.; Peluso, M.A.; Thomas, H.; Damonte, L.C.; Sambeth, J.E. Structural and optical properties of ZnO and manganese-doped ZnO. *J. Alloys Compd.* **2016**, *689*, 416–424. [[CrossRef](#)]
36. Reungoat, J.; Pic, J.S.; Manéro, M.H.; Debellefontaine, H. Adsorption of nitrobenzene from water onto high silica zeolites and regeneration by ozone. *Sep. Sci. Technol.* **2007**, *42*, 1447–1463. [[CrossRef](#)]
37. Staehelin, J.; Hoigne, J. Decomposition of ozone in water: Rate of initiation by hydroxide ions and hydrogen peroxide. *Environ. Sci. Technol.* **1982**, *16*, 676–681. [[CrossRef](#)]
38. Qi, F.; Xu, B.; Chen, Z.; Ma, J.; Sun, D.; Zhang, L. Influence of aluminum oxides surface properties on catalyzed ozonation of 2, 4, 6-trichloroanisole. *Sep. Purif. Technol.* **2009**, *66*, 405–410. [[CrossRef](#)]
39. Altendor, S.; Carene, B.; Emmanuel, E.; Lambert, J.; Ehrhardt, J.; Gaspard, S. Adsorption studies of methylene blue and phenol onto vetiver roots activated carbon prepared by chemical activation. *J. Hazard. Mater.* **2009**, *165*, 1029–1039. [[CrossRef](#)] [[PubMed](#)]
40. Yang, Y.; Ma, J.; Qin, Q.; Zhai, X. Degradation of nitrobenzene by nano-TiO₂ catalyzed ozonation. *J. Mol. Catal. A Chem.* **2007**, *267*, 41–48. [[CrossRef](#)]
41. Zhao, L.; Sun, Z.; Ma, J.; Liu, H. Enhancement mechanism of heterogeneous catalytic ozonation by cordierite-supported copper for the degradation of nitrobenzene in aqueous solution. *Environ. Sci. Technol.* **2009**, *43*, 2047–2053. [[CrossRef](#)] [[PubMed](#)]

42. Zhao, L.; Ma, J.; Sun, Z. Oxidation products and pathway of ceramic honeycomb-catalyzed ozonation for the degradation of nitrobenzene in aqueous solution. *Appl. Catal. B Environ.* **2008**, *79*, 244–253. [[CrossRef](#)]
43. Zhang, T.; Li, C.; Ma, J.; Tian, H.; Qiang, Z. Surface hydroxyl groups of synthetic α -FeOOH in promoting OH generation from aqueous ozone: Property and activity relationship. *Appl. Catal. B Environ.* **2008**, *82*, 131–137. [[CrossRef](#)]



© 2018 by the authors. Licensee MDPI, Basel, Switzerland. This article is an open access article distributed under the terms and conditions of the Creative Commons Attribution (CC BY) license (<http://creativecommons.org/licenses/by/4.0/>).